International Journal of Infectious Diseases xxx (2017) xxx–xxx

Contents lists available at ScienceDirect

International Journal of Infectious Diseases

journal homepage: www.elsevier.com/locate/ijid

Review

Imaging in extrapulmonary tuberculosis

Sanjay Gambhir [a,*], Mudalsha Ravina [a], Kasturi Rangan [a], Manish Dixit [a], Sukanta Barai [a], Jamshed Bomanji [b,*] the International Atomic Energy Agency Extra-pulmonary TB Consortium [1]

[a] Sanjay Gandhi Post Graduate Institute of Nuclear Medicine, Rae Bareli Road, Lucknow, India
[b] Department of Nuclear Medicine, of Nuclear Medicine, UCLH NHS Foundation Trust, 235 Euston Road, London NW1 2BU, UK

ARTICLE INFO

Article history:
Received 12 October 2016
Received in revised form 31 October 2016
Accepted 1 November 2016

Corresponding Editor: Eskild Petersen, Aarhus, Denmark

Keywords:
Tuberculosis
Imaging
CT
PET–CT
MRI
Extrapulmonary tuberculosis
Biomarker
^{18}F-fluorodeoxyglucose (FDG) PET–CT

SUMMARY

Tuberculosis (TB) remains a major global public health problem, with 1.5 million deaths annually worldwide. One in five cases of TB present as extrapulmonary TB (EPTB), posing major diagnostic and management challenges. *Mycobacterium tuberculosis* adapts to a quiescent physiological state and is notable for its complex interaction with the host, producing poorly understood disease states ranging from latent infection to active clinical disease. New tools in the diagnostic armamentarium are urgently required for the rapid diagnosis of TB and monitoring of TB treatments, and to gain new insights into pathogenesis. The typical and atypical imaging features of EPTB are reviewed herein, and the roles of several imaging modalities for the diagnosis and management of EPTB are discussed.

1. Introduction

Tuberculosis (TB) remains a major global public health problem, with 1.5 million deaths annually worldwide (World Health Organization (WHO) 2014). One in five cases of TB present as extrapulmonary TB (EPTB), posing major diagnostic and management challenges. The accurate diagnosis of active pulmonary TB may be challenging in patients without any microbiological evidence of the presence of *Mycobacterium tuberculosis* in sputum samples. The tuberculin skin test (TST) or serum interferon-gamma release assays (IGRAs) can determine TB exposure in such patients, but cannot differentiate between active and latent disease. Culture remains the gold standard, but it can take up to 8–10 weeks for results, and it has been noted that the sensitivity is variable depending on the host and site. Blood culture, urine culture, and the culture of other body fluids mainly aid in the diagnosis.

The most frequent sites of EPTB include the lymph nodes, peritoneum, and the ileocaecal, hepatosplenic, genitourinary, central nervous system (CNS), and musculoskeletal regions; multisystem involvement is common.

Population groups with an increased risk of TB include immunocompromised individuals (AIDS, lymphoma, leukaemia, post-organ transplant), diabetics, children, the elderly, alcoholics, persons with a low socio-economic status, persons with poor compliance, immigrants from developing countries, prisoners, nursing home residents, health care workers, and the homeless.[1–3]

* Corresponding author. Tel.: +91 522 2494623; fax: +91 522 2668017.
E-mail addresses: gaambhir@yahoo.com (S. Gambhir), jamshed.bomanji@nhs.net (J. Bomanji).

[1] The International Atomic Energy Agency Extra-pulmonary TB Consortium: Rajnish Sharma (Molecular Imaging and Research Centre, INMAS, Delhi, India), Bhagwant Rai Mittal (Post Graduate Institute of Medical Education and Research, Chandigarh, India), Sanjay Gambhir (Sanjay Gandhi Post Graduate Institute of Nuclear Medicine, Lucknow, India), Ahmad Qureshy (INMOL Hospital, Lahore, Pakistan), Shamim Momtaz Ferdousi Begum (National Institute of Nuclear Medicine & Allied Sciences, Shahbag, Dhaka), Mike Sathekge (University of Pretoria, Pretoria, South Africa), Mariza Vorster (University of Pretoria, Pretoria, South Africa), Dragana Sobic Saranovic (Nuclear Medicine Clinical Centre of Serbia, Belgrade, Serbia), Pawana Pusuwan (Mahidol University, Bangkok, Thailand), Vera Mann (UCLH NHS Foundation Trust, London, UK), Shobhan Vinjamuri (Royal Liverpool University Hospital, Liverpool, UK), Allimudin Zumla (National Institute of Health Research Biomedical Research Centre at UCL Hospitals, London, UK), Thomas Pascual (International Atomic Energy Agency, Vienna, Austria), Jamshed Bomanji (UCLH NHS Foundation Trust, London, UK).

http://dx.doi.org/10.1016/j.ijid.2016.11.003

Table 1
Comparison of CT, MRI, and ^{18}F-FDG PET–CT in diagnosing EPTB

	CT	MRI	^{18}F-FDG PET–CT
Anatomy	Yes	Yes	Yes
Functionality	No	No	No
Radiation burden	Yes	No	Yes
Treatment response	Yes (size-based)	Yes (size-based)	Both anatomical and functional
Protocol	Regional	Regional	Whole body image in single setting
CNS EPTB	Inferior to MRI	Superior image quality	Fewer lesions detected depending on resolution or if the patient is on steroids
Musculoskeletal TB	Inferior to MRI	Modality of choice	Assessing disease burden and response assessment
Abdominal TB and lymphadenopathy	Modality of choice	-	Response assessment and disease burden

CT, computed tomography; MRI, magnetic resonance imaging; ^{18}F-FDG PET–CT, ^{18}F-fluorodeoxyglucose positron emission tomography–computed tomography; EPTB, extrapulmonary tuberculosis; CNS, central nervous system.

The increase in TB has been witnessed not only in Africa and Asia, but also in European countries. Hence TB remains an important cause of morbidity and mortality worldwide.[4,5]

In this mix of risk factors, multidrug-resistant (MDR)-TB continues to flourish. MDR-TB requires the prolonged administration of toxic second-line drugs, associated with higher morbidity and mortality rates. Patients also remain infectious for a longer period once treatment has been started. A new strain of extensively drug-resistant (XDR)-TB is evolving; this MDR strain is also resistant to second-line drugs including any fluoroquinolone and at least one of three injectable drugs (capreomycin, kanamycin, and amikacin). Despite the enormous burden of disease, current diagnostics are still woefully inadequate to meet research and clinical needs.

Radiological investigations play a crucial role in the early and correct identification of EPTB. Imaging modalities of choice are computed tomography (CT; lymphadenopathy and abdominal TB) and magnetic resonance imaging (MRI; CNS and musculoskeletal TB). MRI is also indicated in paediatric or pregnant patients, in whom radiation is to be avoided. In addition, bone scanning is performed in skeletal TB and ^{18}F-fluorodeoxyglucose (FDG) positron emission tomography–computed tomography (PET–CT) in the assessment of the extent of disease and in monitoring the response to treatment. TB demonstrates a variety of clinical and radiological features depending on the organ site involved and has a known propensity for dissemination from its primary site. Thus, TB can mimic a number of other disease entities, and it is important to be familiar with the various radiological features of TB.

The imaging findings of EPTB and their relevance in the present scenario are illustrated herein. Familiarity with these imaging findings helps in early diagnosis, initiation of therapy, and monitoring of patients on treatment (Table 1).

2. Literature review

A PubMed search for relevant articles discussing the role of imaging in EPTB was performed.

2.1. Tuberculous lymphadenopathy

Also known as scrofula, tuberculous lymphadenopathy is a common form of EPTB seen in endemic populations as well as immunocompromised patients in developed nations. The most commonly affected lymph nodes, in decreasing order, are the cervical (63%), mediastinal (27%), and axillary (8–10%) nodes. Most cases present as unilateral cervical lymphadenopathy.

With regard to imaging features, imaging alone cannot distinguish between the causes of lymphadenopathy.

2.1.1. Ultrasonography

Nodal matting with surrounding oedema is seen. Doppler studies may reveal increased vascularity, mostly at the hilum. This feature allows differentiation from malignant lymph nodes, which show peripheral vascularity.[6]

2.1.2. CT and MRI

The lymph nodes are usually matted. However, density depends on the amount of caseation, which increases with time.[7]

2.1.3. ^{18}F-FDG PET–CT

^{18}F-FDG PET–CT may show peripheral uptake and central hypometabolism, depending on the amount of caseation. ^{18}F-FDG PET–CT has the advantage of identifying all affected lymph node groups within a single setting and allows the selection of the lymph node group most suitable for biopsy (Figure 1).

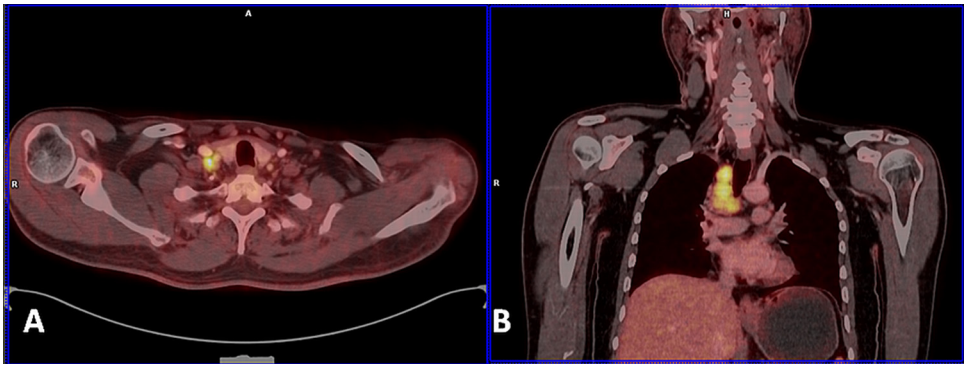

Figure 1. Case of tubercular lymphadenopathy. (A) Transaxial ^{18}F-FDG PET–CT demonstrating a right supraclavicular lymph node with an SUV_{max} of 5.7. (B) Coronal slice revealing multiple mediastinal lymph nodes with an SUV_{max} of 9.9 in the right lower paratracheal region. Hypometabolic areas noted in the nodes are suggestive of caseation/necrosis. The advised site for biopsy was the right supraclavicular lymph node; histopathology subsequently revealed TB. (SUV_{max}, maximum standardized uptake value.).

Please cite this article in press as: Gambhir S, et al. Imaging in extrapulmonary tuberculosis. Int J Infect Dis (2017), http://dx.doi.org/10.1016/j.ijid.2016.11.003

2.2. Abdominal tuberculosis

Abdominal TB may occur directly, as in the case of primary pulmonary TB, or indirectly, via spread from the primary. It generally affects the following organs: lymph nodes, peritoneum, ileocaecal junction, colon, liver, spleen, and adrenal glands.

Solid viscera are affected to a greater extent than the gastrointestinal tract. CT is the mainstay for investigating possible abdominal TB; however, knowledge of other imaging modalities, such as barium enema examination, is important to avoid misdiagnosis in cases in which TB is not initially suspected.

2.3. Abdominal lymphadenopathy

Abdominal lymphadenopathy is the most common manifestation of abdominal TB, seen in 55–66% of patients.[8] On CT, the nodes are usually matted, appearing in groups, with mild fat stranding and a hypoattenuating centre, with or without calcification. ^{18}F-FDG PET–CT shows increased metabolic activity in the nodes and plays a role in the assessment of the response to treatment.

2.4. Peritoneal tuberculosis

Peritoneal TB affects one-third of patients and is one of the most common manifestations of abdominal TB. Subdivision into wet, fibrotic, and dry types has been proposed.[9] On imaging, there may be significant overlap between the three. The wet type manifests in more than 90% of patients and has a high protein and cellular content, leading to high-attenuating pockets of loculated fluid or free ascites. The Hounsfield unit (HU) ranges from 20 to 45. The dry type appears as cake-like omentum with fibrous adhesions and mesenteric thickening. The fibrotic type presents as omental or mesenteric masses.

The main imaging differential diagnoses are malignancy and peritoneal carcinomatosis.[10]

2.5. Gastrointestinal tract tuberculosis

Due to the abundance of lymphoid tissue, the ileocaecal junction (90%) is one of the most common sites of involvement in the bowel.[8,9] The presentation may be ulcerative, hypertrophic, or ulcerohypertrophic.[11,12]

2.5.1. Barium studies

In the early stages, narrowing of the terminal ileum, thickening and gaping of the ileocaecal valve, and thickening and hypermotility of the caecum are noted. In the chronic stages, the ileocaecal valve appears fixed, rigid, and incompetent, while the caecum appears shrunken in size. In the later stages, a 'pulled-up' caecum is usually noted.

2.5.2. CT

On CT, circumferential wall thickening of the terminal ileum and caecum is noted, usually in association with mesenteric lymphadenopathy. The differential diagnosis includes Crohn's disease, carcinoma, and lymphomatous involvement.

Involvement of the oesophagus, stomach, duodenum, and small bowel is still rare. Oesophageal TB is mainly from the carinal lymph nodes. Small bowel TB may present as mucosal thickening. The antrum and distal body are the most commonly affected sites in the stomach. The presence of a fistula or a sinus confirms the diagnosis.

2.6. Hepatosplenic tuberculosis

Hepatosplenic TB may present as miliary or macronodular involvement. The lesions are hypoattenuating on CT and may show peripheral post-contrast enhancement. The most common route of involvement is haematogenous, either through the hepatic artery in military TB or through the portal vein from gastrointestinal lesions. Macronodular involvement is less frequent and is manifested by single or multiple focal density lesions, with or without peripheral rim enhancement.

On MRI, macronodular lesions appear hypointense on T1-weighted images and hypo to hyperintense on T2-weighted images, with thin peripheral and/or internal septal enhancement.

The differential diagnosis includes fungal infections, sarcoidosis, lymphoma, and, rarely, metastasis.

2.7. Adrenal tuberculosis

The adrenal glands are the most common endocrine glands involved by TB. The spread is predominantly via the haematogenous route and may be unilateral or bilateral, with central areas of caseation. Involvement of the adrenal cortex may lead to primary adrenal insufficiency, and where more than 90% of the cortex is involved, a life-threatening addisonian crisis may ensue.[13]

In the early stages, smooth enlargement of the gland with low-density areas and relative central hypoenhancement is noted on CT.[14] In the later stages and/or in previously treated patients, gland atrophy with punctate, localized, or diffuse calcification is observed.

The MRI features are analogous to the CT appearances except for limitations when calcification is present. ^{18}F-FDG PET–CT shows increased metabolic activity in the adrenals in TB or any infection. Often this may be an incidental finding on PET–CT done for another diagnosis. The gland may show diffuse or patchy uptake on ^{18}F-FDG images.

2.8. Genitourinary tuberculosis

TB may involve the genitourinary tract as a secondary site following haematogenous dissemination from the lungs.[15]

2.9. Renal tuberculosis

TB at these sites accounts for 15–20% of cases of EPTB.[16] Two morphological appearances are seen routinely: pyelonephritis or a pseudotumoural type presenting as single or multiple nodules.

The collecting system is involved in isolation or due to contiguous spread from the parenchyma. In the early stages, papillary necrosis resulting in uneven caliectasis is noted. Hydronephrosis and multifocal strictures with mural thickening and enhancement are observed in progressive disease. Progressive hydronephrosis and parenchymal thinning with dystrophic calcification are noted in end-stage disease.

2.9.1. Plain radiography

On plain radiographs, foci of calcification are noted in 25–45% of patients.[17] Triangular ring-like calcification in the collecting system is observed in cases of papillary necrosis. Amorphous focal ground glass-like calcification (putty kidney) is seen in end-stage disease.[18]

2.9.2. Intravenous urography

Plain film intravenous urography is quite sensitive in detecting renal TB:[19] only 10–15% of those affected have normal imaging. A range of findings may be observed, including parenchymal scars (50%), moth-eaten calyces due to necrotizing papillitis, irregular caliectasis, phantom calyx, and hydronephrosis. Lower urinary tract signs include the 'Kerr kink', which occurs due to abrupt narrowing at the pelviureteric junction.[20]

Please cite this article in press as: Gambhir S, et al. Imaging in extrapulmonary tuberculosis. Int J Infect Dis (2017), http://dx.doi.org/10.1016/j.ijid.2016.11.003

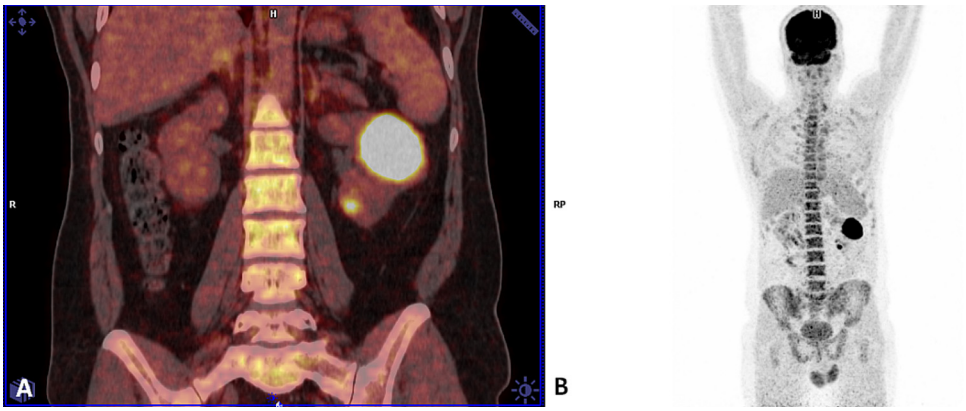

Figure 2. Case of tubercular pyelonephritis. (A) Coronal fused ^{18}F-FDG PET–CT images showing two lesions in the middle and the lower pole of the left kidney. (B) Maximum intensity projection image revealing two foci in the left kidney with no other lesion detected elsewhere in the body.

2.9.3. Ultrasonography

In early-stage disease, ultrasonography may show an irregular cortical outline with calcification. As the disease progresses, papillary destruction with echogenic masses and distorted renal parenchyma can be observed. In end-stage disease, heavy dystrophic calcification with a small shrunken kidney is noted.

Ultrasonography is less sensitive in detecting isoechoic masses and small calcifications and in identifying small cavities communicating with the collecting system.

2.9.4. CT and MRI

CT intravenous pyelography is most sensitive in identifying all manifestations of renal TB. Depending on the site of the stricture, various patterns of hydronephrosis may be seen, including focal caliectasis, caliectasis without pelvic dilatation, and generalized hydronephrosis. Other common findings include parenchymal scarring and low-attenuation parenchymal lesions. CT is also useful in depicting the extension of disease into the extrarenal space.[21,22]

The radiological differential diagnosis of renal TB includes other causes of papillary necrosis, transitional cell carcinoma, and other infections. ^{18}F-FDG PET–CT may be used to evaluate renal masses (Figure 2), to identify latent or active TB in the lung, or to monitor therapy.

2.10. Ureteric tuberculosis

2.10.1. Intravenous urography

In the chronic state, beaded areas due to alternate strictures and dilatation are noted.

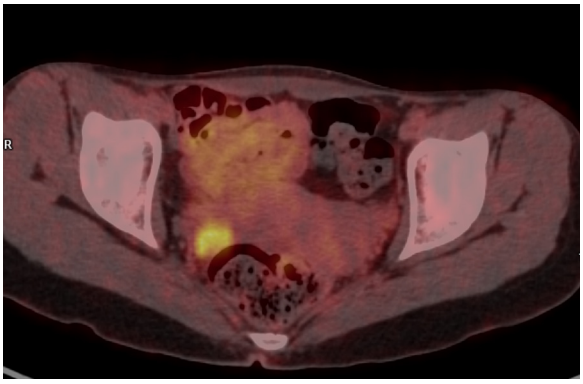

Figure 3. ^{18}F-FDG-avid lesion in the right adnexa (SUV_{max} 4.4). (SUV_{max}, maximum standardized uptake value).

2.10.2. CT

Ureteral wall thickening is observed in the acute setting. In chronic disease, strictures and shortening of the ureter, leading to pipe stem ureter, are noted.

2.11. Urinary bladder tuberculosis

Urinary bladder involvement is secondary to the descending spread of infection along the urinary tract.[22] An irregular wall with a small capacity bladder is noted. Fibrotic changes at the ureteric orifices lead to vesicoureteric reflux and hydroureteronephrosis.[23]

2.12. Female genital organs

Involvement of the genital organs occurs in 1.5% of females affected with TB. Spread may be via the haematogenous or lymphatic route. On hysterosalpingography, obstruction is usually noted at the junction of the isthmus and the ampulla.[24,25] A beaded appearance is seen due to multiple constrictions. A normal uterine cavity may be observed in more than 50% of cases. A further possible presentation is as an irregular filling defect with uterine synechiae and shrunken cavity (3–18% of cases). Lesions may show uptake on ^{18}F-FDG PET–CT (Figure 3).

2.13. Male genital organs

Involvement of the genital organs in males is generally confined to the seminal vesicles or prostate gland, with occasional calcification (10% of cases). The testes and epididymides are rarely involved. Hypoattenuating lesions are noted on contrast-enhanced CT, likely representing foci of caseous necrosis. Non-tuberculous pyogenic prostatic abscesses have a similar CT appearance.[22] The spread is haematogenous and self-limiting. Ultrasonography shows focal or diffuse areas of decreased echogenicity; however, these findings are very non-specific.[23,26]

2.14. Musculoskeletal tuberculosis

Musculoskeletal TB accounts for about 3% of all TB infections. The main route of spread is haematogenous, from lungs, or via activation of dormant infection in bone or joint post-trauma.[27] Cases of musculoskeletal TB are usually subclassified as tubercular spondylitis (50%) (popularly called Potts' spine), peripheral tuberculous arthritis (60%), osteomyelitis (38%), and soft tissue TB, including tenosynovitis and bursitis.[28–30]

Please cite this article in press as: Gambhir S, et al. Imaging in extrapulmonary tuberculosis. Int J Infect Dis (2017), http://dx.doi.org/10.1016/j.ijid.2016.11.003

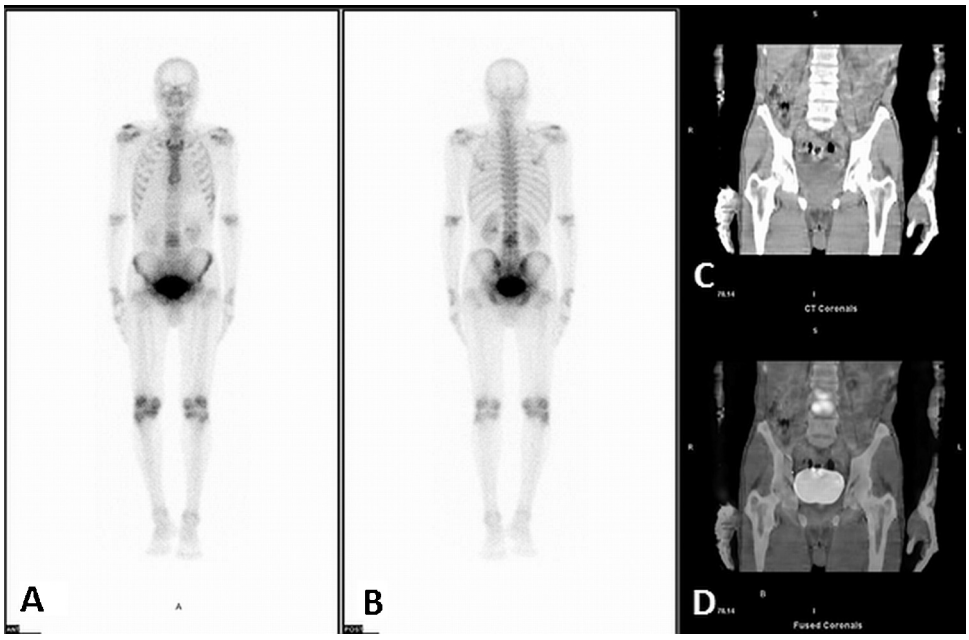

Figure 4. (A) and (B) ^{99m}Tc-MDP bone scan (anterior and posterior views) revealing increased tracer uptake in L3–4 vertebrae; (C) and (D) with soft tissue component noted on SPECT-CT and CT images. (^{99m}Tc-MDP, 99m-technetium methylene diphosphonate; SPECT, single-photon emission computed tomography; CT, computed tomography).

2.15. Tubercular spondylitis

The disease spread is via the venous plexus of Batson. The most commonly affected vertebrae are the lower thoracic and upper lumbar. The vertebral body is involved to a greater extent than the posterior elements, and the classical presentation is involvement of two or more contiguous vertebrae, with or without paravertebral abscess. The presence of calcification, which may sometimes be absent, almost confirms the diagnosis. In cases of anterior subligamentous involvement, the infection spreads inferiorly or superiorly without vertebral disc involvement.

2.15.1. Plain radiography

Potential early changes include irregular end-plates and a decrease in vertebral height. Sharp angulation or gibbus deformity is noted, with anterior wedging or collapse. The displacement of paraspinal lines suggestive of psoas involvement may be noted. The calcified psoas is suggestive of an abscess.

Spinal TB might lead to vertebra plana where there is a reduction in anterior and posterior height, preserved intervertebral disc, and some forms of vertebral end-plate change.

2.15.2. Ultrasonography

Ultrasonography is usually helpful in identifying iliopsoas abscess and its percutaneous drainage.

2.15.3. CT

Cross-sectional imaging is required to better establish the extent of vertebral involvement and the possible presence of a paravertebral abscess.

2.15.4. MRI

MRI is the gold standard investigation for tubercular spondylitis. MRI helps to identify the presence of an epidural component and cord compression. An early finding is focal T2 hyperintense and T1 hypointense bone marrow oedema in the anterior part of vertebral body adjacent to the end-plates, with patchy post-contrast enhancement. An abnormal T2 hyperintense signal is noted in the involved disc space, with reduced height. Multifocal TB, compression of the spinal cord, abnormal T2 hyperintense signal in the spinal cord, and neural foraminal and neural compromise secondary to epidural collections are well demonstrated on MRI. MRI may also demonstrate the complete extent of an iliopsoas or paraspinal abscess. Small foci of involvement of posterior elements are better observed on MRI than CT.[31–33]

2.15.5. Bone scintigraphy

A ^{99m}Tc-methylene diphosphonate bone scan may identify multifocal sites and can sometimes be used to rule out metastasis suggested by the involvement of multiple contiguous vertebrae (Figure 4).

2.15.6. ^{18}F-FDG PET–CT

^{18}F-FDG PET–CT may show increased uptake in tubercular spondylitis, with the identification of multiple sites, and offers further help in monitoring the response to treatment[34,35] (Figures 5 and 6).

2.16. Tubercular arthritis

Tubercular arthritis is the most common extra-axial form of musculoskeletal TB. It is monoarticular in 90% of cases, commonly affecting the large weight-bearing joints such as the hip and knee.[36,37] Less commonly it involves the shoulder, elbow, and sacroiliac joints. Peri-articular osteoporosis, peripherally located osseous erosion, and progressive decrease in the joint space suggest the diagnosis of TB and are popularly referred to as the 'Phemister triad'. In the later stages, fibrosing ankylosis ensues.[37–39] Atrophic changes in bones may occur and lead to atrophic arthropathy, especially in the shoulder joint.

2.16.1. Ultrasonography

Ultrasonography mainly helps in identifying joint effusion, although the appearances are non-specific.

2.16.2. CT

CT helps to establish the degree of bone destruction. Sequestrum or sinus formation can be demonstrated on post-contrast scan.

Please cite this article in press as: Gambhir S, et al. Imaging in extrapulmonary tuberculosis. Int J Infect Dis (2017), http://dx.doi.org/10.1016/j.ijid.2016.11.003

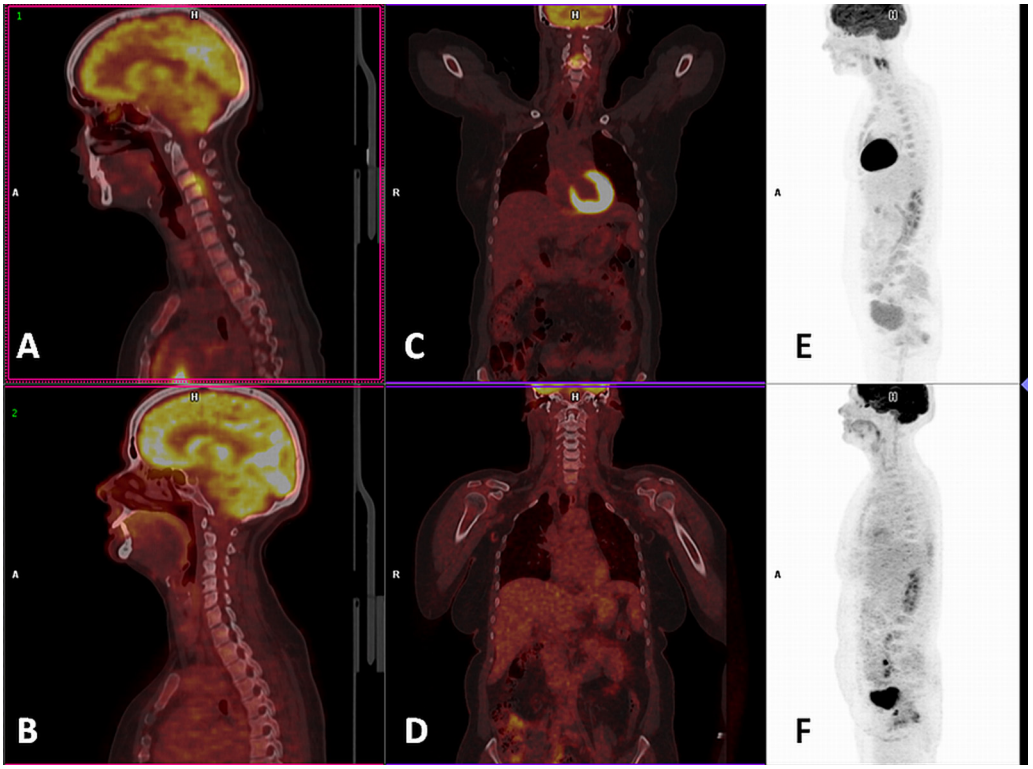

Figure 5. Case of cervical spondylitis. Pre-treatment ^{18}F-FDG PET–CT: (A) sagittal view; (C) coronal view; (E) MIP, showing contiguous involvement of the C3/C4 vertebrae with a paravertebral component and an SUV_{max} of 4.4. The corresponding post-treatment PET–CT after 6 months: (B), (D), and (F), showing a complete metabolic response. (MIP, maximum intensity projection; SUV_{max}, maximum standardized uptake value).

2.16.3. MRI

Lesions are usually T1 hyperintense and T2 hypointense and show brilliant post-gadolinium enhancement, which is a result of blood degradation products and inflammation. Sinus tracts appear as linear T2 hyperintensity with marginal 'tram track enhancement'.[28,37]

2.17. Tubercular osteomyelitis

Tubercular osteomyelitis is most commonly seen in bones of the extremities (femur, tibia), including the small bones of the hands and feet (Figures 7 and 8), often involving the epiphyses. In children, metaphyseal foci can involve the growth plate, a feature that differentiates TB from pyogenic infection.[40] Radiologically, foci of osteolysis with varying degrees of eburnation and periostitis are observed.

2.18. Tubercular dactylitis

Tuberculous dactylitis, in which there is painless involvement of the short tubular bones of the hands and feet, is more common in children. At radiography, pronounced fusiform soft tissue swelling with or without periostitis is the most common finding.[41,42]

2.19. CNS tuberculosis

The spread is either haematogenous, or by direct extension from local infection, such as tuberculous otomastoiditis. CNS TB accounts for 1% of all TB and 10–15% of EPTB. It is a leading cause of morbidity and mortality in endemic regions.[43,44]

Manifestations of cranial TB include (1) extra-axial: tubercular leptomeningitis and tubercular pachymeningitis, (2) intra-axial: tuberculoma, focal cerebritis, tubercular abscess, tubercular rhomboencephalitis, and tubercular encephalopathy.

2.20. Tubercular leptomeningitis

Tubercular leptomeningitis (TBM) is more common than pachymeningitis. It presents with thick tuberculous exudate in the base of the brain in the subarachnoid space, the most common location being the interpeduncular fossa. Extension to the surface of the cerebral hemispheres is rare.

Cerebrospinal fluid (CSF) flow may be disrupted, leading to obstructive hydrocephalus or communicating hydrocephalus due to obstruction in the basal cisterns. Ischemic infarcts due to arteritis are also noted. In addition, involvement of the cranial nerves may be observed, with the second, third, fourth, and seventh most frequently affected.[45–47]

On MRI, abnormal meningeal enhancement is noted. The magnetization transfer (MT) technique is reported to be superior in differentiating TBM from other causes of meningitis. The meninges appear hyperintense on pre-contrast T1-weighted MT images and enhance further on post-contrast T1-weighted MT images. The MT ratio in TBM is significantly higher than in viral meningitis, while fungal and pyogenic meningitis show a higher MT ratio compared with TBM.[48]

2.21. Tubercular pachymeningitis

Tubercular pachymeningitis is rare and is characterized by plaque-like regions of pachymeningeal enhancement that appear hyperdense on plain CT scan, isointense to brain on T1-weighted imaging, and isointense to hypointense on T2-weighted imaging. Homogeneous post-contrast scan enhancement is noted.

2.22. Tuberculoma

Lesions may be solitary, multiple, or miliary. The most commonly affected areas are the frontal and parietal lobes.

Please cite this article in press as: Gambhir S, et al. Imaging in extrapulmonary tuberculosis. Int J Infect Dis (2017), http://dx.doi.org/10.1016/j.ijid.2016.11.003

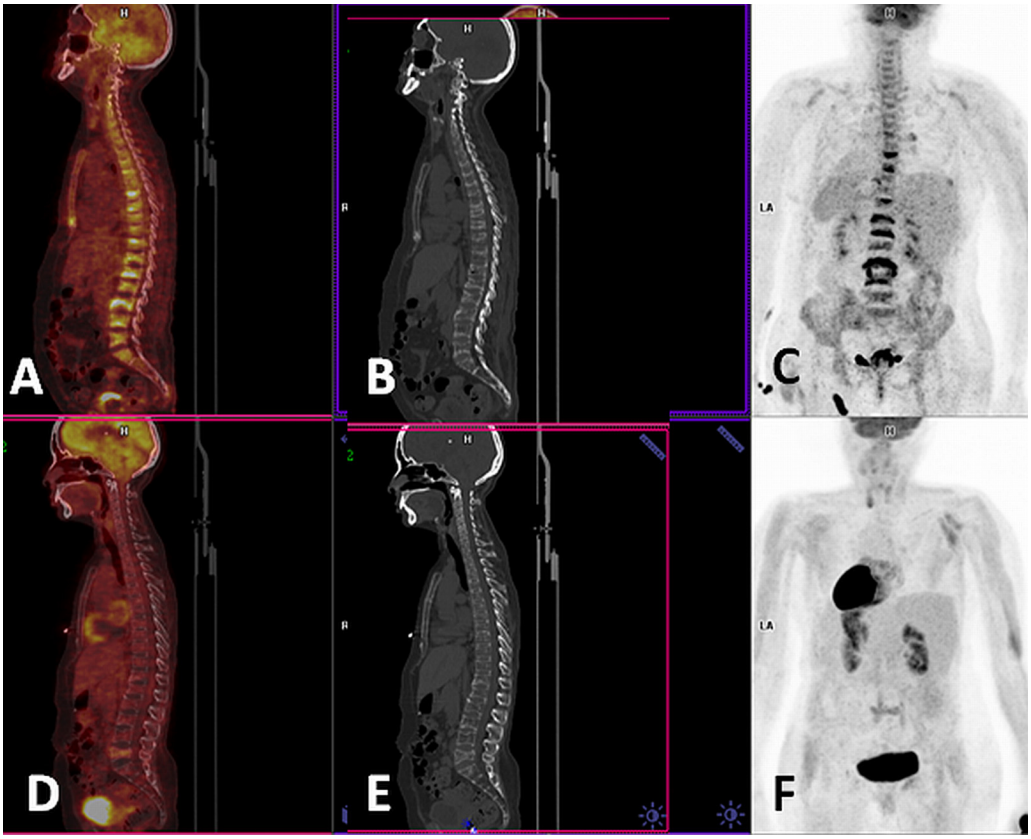

Figure 6. Case of tubercular spondylitis. Pre-treatment scans: (A) sagittal ^{18}F-FDG PET–CT and (C) MIP; (B) CT showing disco-vertebral changes with partial collapse in multiple dorsal lumbar vertebrae. Post-treatment scans: (D), (E), (F) showing near-complete resolution of all lesions except for mild tracer uptake in the L3 vertebra.

Tuberculomas account for 15–50% of space-occupying lesions in endemic areas.

2.22.1. CT

The classical presentation is homogeneous ring-enhancing lesions with irregular walls of varying thickness. One-third of patients demonstrate the 'target sign' (i.e., central calcification or punctate enhancement with surrounding hypoattenuation and ring enhancement).[45]

2.22.2. MRI

Appearances on MRI depend on whether the tuberculoma is caseating or non-caseating. Non-caseating tuberculomas are hypointense on T1-weighted and hyperintense on T2-weighted images, with homogeneous post-contrast enhancement. Caseating granulomas are isointense to hypointense on both T1- and T2-weighted images, with peripheral post-contrast enhancement. Caseating granuloma may show central T2 hyperintensity owing to liquefaction. Associated TBM may be seen. In miliary TB, tiny 2- to 5-mm T2 hyperintense disc-enhancing tuberculomas are seen with TBM. They are better visualized on MT spin echo T1-weighted images.[49] Magnetic resonance spectroscopy is promising in the specific diagnosis of tuberculomas. A large lipid lactate peak at 1.3 ppm is characteristic, with associated reduced *N*-acetyl aspartate and/or slightly increased choline levels.

^{18}F-FDG PET–CT and MRI might be complementary to each other in identifying the lesions (Figure 9).

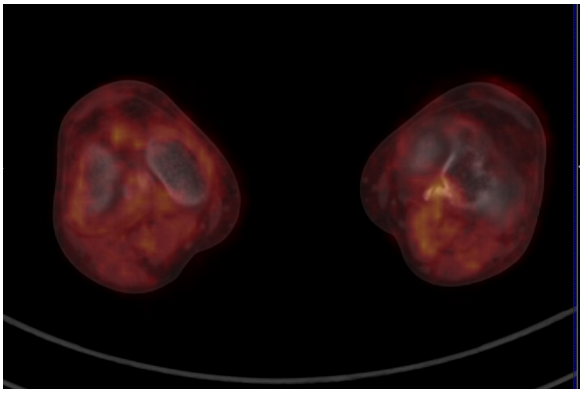

Figure 7. An ^{18}F-FDG-avid lesion is noted in the lateral aspect of the medial condyle of the left femur, which is a rare involvement in TB osteomyelitis.

2.23. Tubercular abscess

Tubercular abscess accounts for 4–7% of cases in the endemic region. Presentation is as a large solitary lesion, which may be multi-loculated, with surrounding vasogenic oedema and mass effect. Such abscesses have pus-filled centres and vascular granulation tissue, and demonstrate an absence of epithelioid granulomatous reaction. The causative organism may be isolated from the pus, in contrast to tuberculomas.

The lesion may show central low intensity on T1-weighted images and peripheral low intensity due to vasogenic oedema. Diffusion-weighted imaging reveals restricted diffusion with low apparent diffusion coefficient values. On imaging, pyogenic and fungal abscesses may mimic tuberculous abscess. Tuberculous abscess shows a large lipid lactate peak at 1.3 ppm on magnetic resonance spectroscopy owing to the presence of mycolic acid within the mycobacterial walls, which represents a distinguishing feature from pyogenic abscess.[50]

Please cite this article in press as: Gambhir S, et al. Imaging in extrapulmonary tuberculosis. Int J Infect Dis (2017), http://dx.doi.org/10.1016/j.ijid.2016.11.003

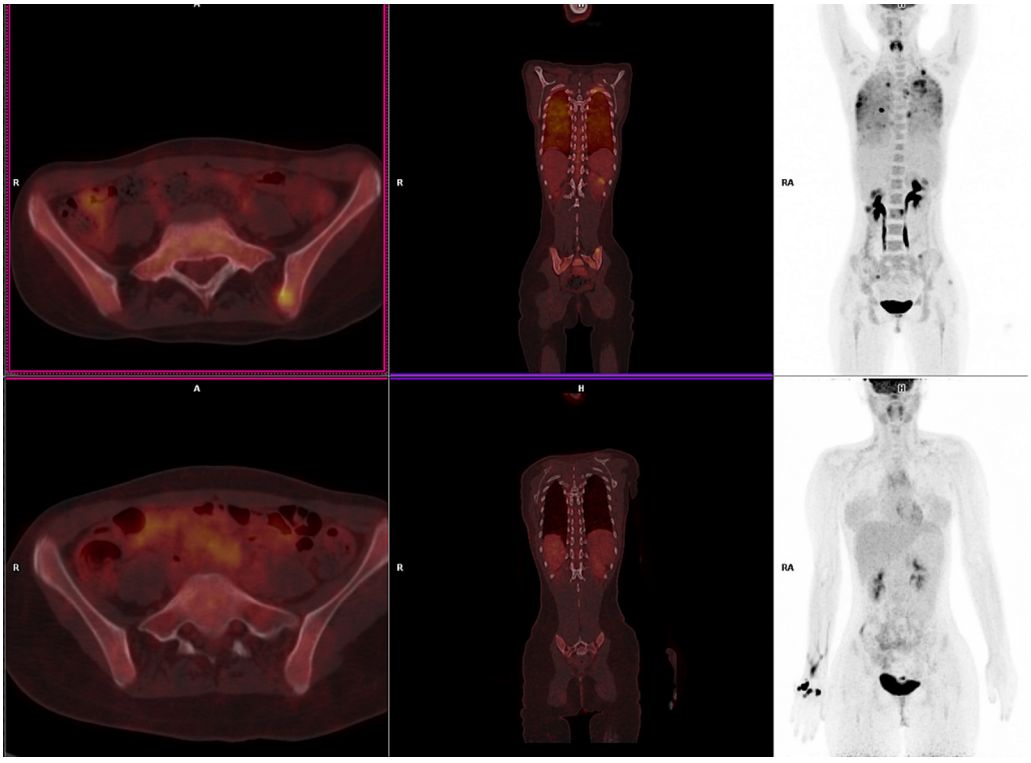

Figure 8. Prior to treatment, ^{18}F-FDG-avid lesions are noted in both lungs and the left iliac bone adjoining the sacrum (top row). After appropriate treatment, complete metabolic resolution of both lesions (bottom row).

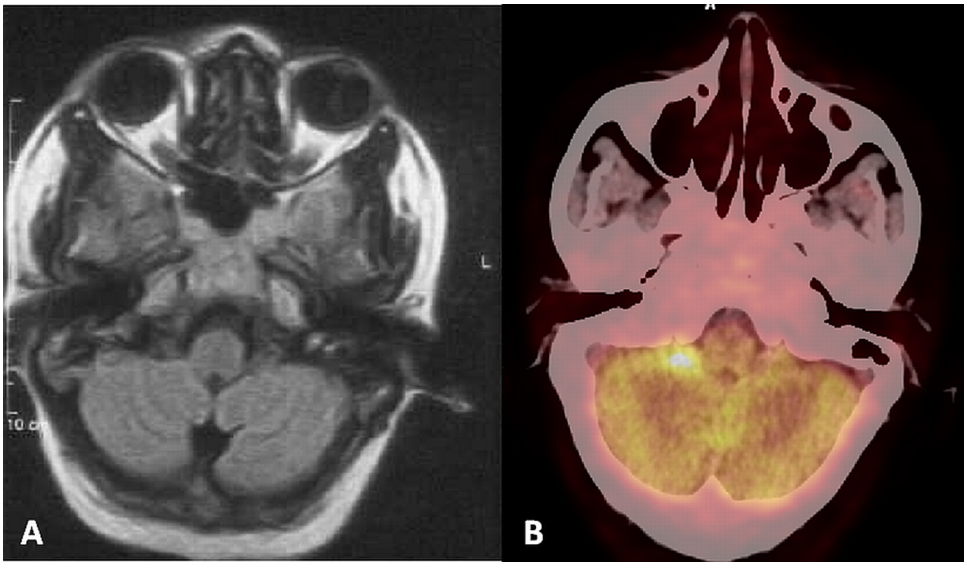

Figure 9. Case of tubercular meningitis. A solitary ^{18}F-FDG-avid lesion was seen in the right anterior cerebellum (B), which was missed on MRI (A), demonstrating that these modalities may be complementary in identifying brain lesions.

2.24. Rhomboencephalitis

Rhomboencephalitis is a particular form of neurotuberculosis affecting the hind brain. The most common manifestation is tuberculoma.

2.25. Encephalopathy

Encephalopathy in the context of TB is most commonly observed in children and infants with pulmonary TB. The postulated mechanism is a delayed type IV hypersensitivity reaction initiated by a tuberculous protein, which leads to extensive damage of the white matter with infrequent perivascular demyelination. Imaging shows extensive unilateral or bilateral brain oedema.[51]

2.26. Spinal and meningeal involvement

Spinal TB (Figure 10) commonly manifests as TBM and rarely as intramedullary tuberculoma. MRI is the modality of choice for the

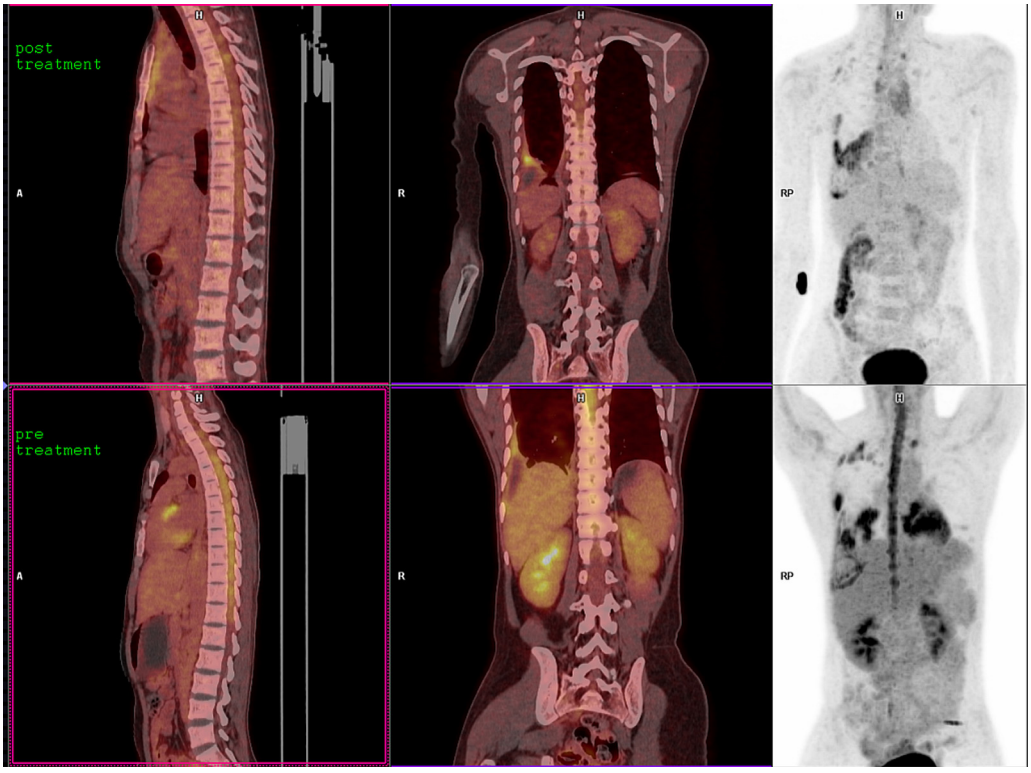

Figure 10. ^{18}F-FDG-avid lesion noted along the entire spinal canal prior to treatment (bottom row). The lesion has entirely disappeared following treatment (top row).

assessment of spinal TB. Spinal TBM manifests as linear enhancing exudates along the spinal cord in the subarachnoid spaces and clumping of cauda equina nerve roots.[34]

2.27. Tubercular otomastoiditis

Tubercular otomastoiditis, which occurs acutely secondary to TB infection, is more frequently observed in immunocompromised patients. It may present with painless chronic otorrhoea with an intact tympanic membrane, or as pain, purulent discharge, and ossicular erosion. There may be associated cervical lymph node involvement in the interparotid, upper cervical, and pre-auricular regions. Pachymeningeal involvement with potential dural sinus thrombosis is also sometimes seen.

2.28. Tubercular mastitis

Tubercular mastitis is a rare occurrence, although the incidence has been rising (0.1–3%) in endemic areas like Africa and India.[52] The first case was reported in 1829 by Sir Ashley Cooper, who referred to it as "scrofulous swelling of the bosom".[53] The significance of breast TB lies in the fact that it masquerades the symptoms of breast cancer and inflammatory disease of the breast. It may present in nodular form or as multifocal disease.[53] Radiological imaging is not diagnostic, as there is significant overlap with other pathologies. Breast ultrasonography may show a hypoechoic mass or focal or sectorial duct ectasia. Caseating granulomas in a tissue sample are diagnostic.

2.29. Cardiac tuberculosis

Cardiac TB is a rare infection involving the cardiac muscles that is seen in 1–2% of patients with pulmonary TB.[54,55] There is predominantly pericardial and myocardial involvement, and endocardial spread may occur from the myocardium.

2.29.1. Plain radiography

The radiographic appearance may be normal in the early stages, while pericardial calcification may be evident in the later stages.

2.29.2. CT and MRI

CT may reveal pericardial effusion, thickening, or calcification in the chronic stages. On cardiac MRI, T1-weighted images may show a nodular lesion that appears isointense to slightly hyperintense. On T2-weighted images the lesion appears isointense, with mild enhancement post gadolinium.

2.30. Role of PET–CT: challenges and limitations

FDG is a non-physiological glucose analogue that undergoes metabolism by the same physiological processes as glucose, including being taken up by cell surface transporters (mainly the glucose transporter-1, GLUT-1) and transformed by the rate-limiting glycolytic enzyme, hexokinase, into FDG-6-phosphate. An interesting early observation by Kubota et al. was that a substantial component of ^{18}F-FDG uptake in tumour tissue is a result of activity localizing to peritumoural inflammatory cells, such as macrophages, which demonstrate greater ^{18}F-FDG uptake than tumour cells.[56] Multiple mechanistic similarities are now recognized between inflammatory and malignant cells in terms of the underlying metabolic pathways.[56] It is this differential increase in tissue glycolysis in inflamed tissue, as opposed to normal cells, that forms the pathophysiological basis for the use of ^{18}F-FDG PET–CT in TB.

^{18}F-FDG PET–CT is useful in identifying the extent of disease in patients with EPTB. Tubercular lymphadenopathy shows high-grade metabolism, and ^{18}F-FDG PET–CT may therefore help in selecting nodes suitable for biopsy based on metabolic uptake/standardized uptake values (SUVs). Moreover, PET–CT is more sensitive than structural imaging methods in detecting lesions.

Apart from assisting in the selection of the site for biopsy, PET–CT may play a significant role in monitoring the response to

Please cite this article in press as: Gambhir S, et al. Imaging in extrapulmonary tuberculosis. Int J Infect Dis (2017), http://dx.doi.org/10.1016/j.ijid.2016.11.003

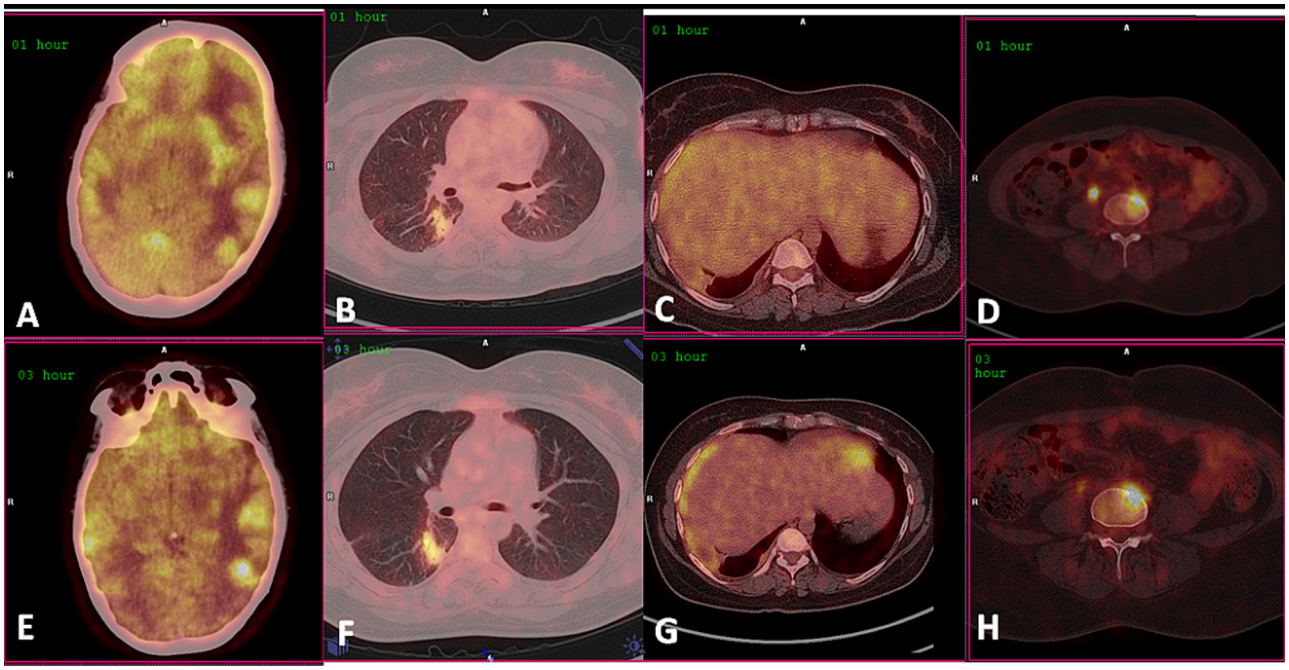

Figure 11. Dual time-point imaging of the patient at 1 h ((A)–(D)) and 3 h ((E)–(H)), showing a substantial increase in lesion contrast.

treatment: its ability to detect changes in metabolic uptake means that it may be considered a specific complementary tool to structural imaging for this purpose.[57] The refining of imaging techniques like dual time-point imaging may further improve the detection of disease[60,61] (Figure 11).

Repeat biopsy in bone TB is not advised, and in this context metabolic uptake on ^{18}F-FDG PET–CT may be taken into consideration. Indeed, ^{18}F-FDG PET–CT represents an ideal non-invasive modality for the assessment of the response to treatment and disease activity. In patients with increased metabolic uptake on treatment, this most likely suggests disease progression or an increased disease burden. In such cases, the patient might benefit from a prolongation of treatment duration/change of drug regime, thus individualizing the treatment protocol.[57–59]

2.31. TB associated with HIV infection

The immunocompromised status associated with HIV infection reduces the threshold for reactivation of dormant diseases such as TB. In such patients, the treatment of TB goes hand in hand with HIV treatment and can be similarly followed up with serial PET–CT scans. However, frequent monitoring is essential in these cases, as faster conversion of bacteria into resistant forms is often seen.[60]

With the increase in XDR and MDR-TB and HIV infection, an individualized therapeutic approach is gaining greater importance in this chronic inflammatory disease, which requires a sensitive diagnostic method for the assessment of not only treatment efficacy, but also initial disease spread, as well as for guidance of biopsy when equivocal findings are observed.

Patients with HIV and TB are prone to developing certain concomitant malignant lesions. As mentioned previously, the major limitation of PET in this context is that it cannot adequately differentiate the aetiology of various lesions/lymph nodes.

3. Conclusions

Radiological investigations continue to play an important role in the evaluation of various manifestations, sites of infection, and disease burden in patients with TB, especially EPTB, bearing in mind that TB can mimic a number of other disease entities.

The authors understand that biopsy and culture studies remain the gold standard for diagnosing TB. FDG PET–CT provides a visual metabolic map, complementary to conventional imaging techniques. Also, whole-body PET–CT imaging may shorten the time period involved in assessing the disease burden and may play an important role in decision-making regarding the duration of therapy, especially in developing countries in those with EPTB. More precise characterization of the role of PET–CT in clinical management decision-making awaits further studies involving larger numbers of patients.

Acknowledgements

All authors are grateful to the International Atomic Energy Agency for their support of the Coordinated Research Project (CRP) E15021.

Conflict of interest: None.

References

1. World Health Organization. Global tuberculosis report 2015, 20th ed., Geneva: WHO; 2015.
2. Maclean KA, Becker AK, Chang SD, Harris AC. Extrapulmonary tuberculosis: imaging features beyond the chest. *Can Assoc Radiol J* 2013;**64**:319–24.
3. Rafique A. The spectrum of tuberculosis presenting at a London district general hospital. *West Lond Med J* 2009;**1**:19–38.
4. Alrajhi AA, Al-Barrak AM. Extrapulmonary tuberculosis, epidemiology and patterns in Saudi Arabia. *Saudi Med J* 2002;**23**:503–8.
5. Zumla A. The white plague returns to London—with a vengeance. *Lancet* 2011;**377**:10–1.
6. Ahuja A, Ying M, Yuen YH, Metreweli C. Power Doppler sonography to differentiate tuberculous cervical lymphadenopathy from nasopharyngeal carcinoma. *AJNR Am J Neuroradiol* 2001;**22**:735–40.
7. Lee JK. Computed body tomography with MRI correlation. Philadelphia: Lippincott Williams & Wilkins; 2006.
8. Leder RA, Low VH. Tuberculosis of the abdomen. *Radiol Clin North Am* 1995;**33**:691–705.
9. Suri S, Gupta S, Suri R. Computed tomography in abdominal tuberculosis. *Br J Radiol* 1999;**72**:92–8.
10. Takalkar AM, Bruno GL, Reddy M, Lilien DL. Intense FDG activity in peritoneal tuberculosis mimics peritoneal carcinomatosis. *Clin Nucl Med* 2007;**32**:244–6.

11. Thoeni R, Margulis A. Gastrointestinal tuberculosis. *Semin Roentgenol* 1979;**14**:283–94.
12. Nakano H, Jaramillo E, Watanabe M, Miyachi I, Takahama K, Itoh M. Intestinal tuberculosis: findings on double contrast barium enema. *Gastrointest Radiol* 1992;**17**:108–14.
13. Huang YC, Tang YL, Zhang XM, Zeng NL, Li R, Chen TW. Evaluation of primary adrenal insufficiency secondary to tuberculosis adrenalitis with computed tomography and magnetic resonance imaging: current status. *World J Radiol* 2015;**7**:336–42.
14. Buxi TB, Vohra RB, Sujatha, Byotra SP, Mukherji S, Daniel M. CT enlargement due to tuberculosis: a review of literature with five new cases. *Clin Imaging* 1992;**16**:102–8.
15. Pasternak MS, Rubin RH. Urinary tract tuberculosis. In: Schrier RW, editor. *Diseases of the kidney and urinary tract*. 7th ed., Philadelphia: Lippincott Williams & Wilkins; 2001. p. 1017–37.
16. Burrill J, Williams CJ, Bain G, Conder G, Hine AL, Misra RR. Tuberculosis: a radiologic review. *Radiographics* 2007;**27**:1255–73.
17. Kollins SA, Hartman GW, Carr DT, Segura JW, Hattery RR. Roentgenographic findings in urinary tract tuberculosis: a 10 year review. *Am J Roentgenol Radium Ther Nucl Med* 1974;**121**:487–99.
18. Davidson AJ, Hartman DS, Choyke PL, Wagner BJ. Parenchymal disease with normal size and contour. In: Davidson AJ, editor. *Davidson's radiology of the kidney and genitourinary tract*. 3rd ed., Philadelphia: Saunders; 1999. p. 327–58.
19. Kenney PJ. Imaging of chronic renal infections. *AJR Am J Roentgenol* 1990;**155**:485–94.
20. Berry M. Diagnostic radiology, urogenital imaging. New Delhi: Jaypee Brothers Publishers; 2003.
21. Wang LJ, Wong YC, Chen CJ, Lim KE. CT features of genitourinary tuberculosis. *J Comput Assist Tomogr* 1997;**21**:254–8.
22. Harisinghani MG, McLoud TC, Shepard JA, Ko JP, Shroff MM, Mueller PR. Tuberculosis from head to toe. *Radiographics* 2000;**20**:449–70.
23. Kim SH. Genitourinary tuberculosis. In: Pollack HM, Dyer R, McClennan BL, editors. *Clinical urography*. 2nd ed., Philadelphia: Saunders; 2000. p. 1193–228.
24. Jung YY, Kim JK, Cho KS. Genitourinary tuberculosis: comprehensive cross-sectional imaging. *AJR Am J Roentgenol* 2005;**184**:143–50.
25. Sharma JB, Pushpraj M, Roy KK, Neyaz Z, Gupta N, Jain SK, et al. Hysterosalpingographic findings in infertile women with genital tuberculosis. *Int J Gynaecol Obstet* 2008;**101**:150–5.
26. Michaelides M, Sotiriadis C, Konstantinou D, Pervana S, Tsitouridis I. Tuberculous orchitis US and MRI findings: correlation with histopathological findings. *Hippokratia* 2010;**14**:297–9.
27. Andronikou S, Bindapersad M, Govender N, Waner JI, Segwe A, Palliam S, et al. Musculoskeletal tuberculosis—imaging using low-end and advanced modalities for developing and developed countries. *Acta Radiol* 2011;**52**:430–41.
28. Suh JS, Lee JD, Cho JH, Kim MJ, Han DY, Cho NH. MR imaging of tuberculous arthritis: clinical and experimental studies. *J Magn Reson Imaging* 1996;**6**:185–9.
29. Jaovisidha S, Chen C, Ryu KN, Siriwongpairat P, Pekanan P, Sartoris DJ, et al. Tuberculous tenosynovitis and bursitis: imaging findings in 21 cases. *Radiology* 1996;**201**:507–13.
30. Martini M, Adjrad A, Boudjemaa A. Tuberculous osteomyelitis: a review of 125 cases. *Int Orthop* 1986;**10**:201–7.
31. Lee KY. Comparison of pyogenic spondylitis and tuberculous spondylitis. *Asian Spine J* 2014;**8**:216–23.
32. Sinan T, Al-Khawari H, Ismail M, Ben-Nakhi A, Sheikh M. Spinal tuberculosis: CT and MRI feature. *Ann Saudi Med* 2004;**24**:437–41.
33. Raut AA, Naphade PS, Ramakantan R. Imaging spectrum of extrathoracic tuberculosis. *Radiol Clin North Am* 2016;**54**:475–501.
34. Bomanji JB, Gupta N, Gulati P, Das CJ. Imaging in tuberculosis. *Cold Spring Harb Perspect Med* 2015;**5**:a017814.
35. Skoura E, Zumla A, Bomanji J. Imaging in tuberculosis. *Int J Infect Dis* 2015;**32**:87–93.
36. De Backer AI, Mortelé KJ, Vanhoenacker FM, Parizel PM. Imaging of extraspinal musculoskeletal tuberculosis. *Eur J Radiol* 2006;**57**:119–30.
37. De Backer AI, Vanhoenacker FM, Sanghvi DA. Imaging features of extraaxial musculoskeletal tuberculosis. *Indian J Radiol Imaging* 2009;**19**:176–86.
38. Dhillon MS, Sharma S, Gill SS, Naqi ON. Tuberculosis of bones and joints of the foot: an analysis of 22 cases. *Foot Ankle* 1993;**14**:505–13.
39. Hugosson C, Nyman RS, Brismar J, Larsson SG, Lindahl S, Lundstedt C. Imaging of tuberculosis. V. Peripheral osteoarticular and soft-tissue tuberculosis. *Acta Radiol* 1996;**37**:512–6.
40. Lee AS, Campbell JA, Hoffman EB. Tuberculosis of the knee in children. *J Bone Joint Surg Br* 1995;**77**:313–8.
41. Bhaskar, Khonglah T, Bareh J. Tuberculous dactylitis (spina ventosa) with concomitant ipsilateral axillary scrofuloderma in an immunocompetent child: a rare presentation of skeletal tuberculosis. *Adv Biomed Res* 2013;**2**:29.
42. Singhal S, Arbart A, Lanjewar A, Ranjan R. Tuberculous dactylitis—a rare manifestation of adult skeletal tuberculosis. *Indian J Tuberc* 2005;**52**:218–9.
43. Garg RK. Classic diseases revisited: tuberculosis of the central nervous system. *Postgrad Med J* 1999;**75**:133–40.
44. Thwaites GE, Tran TH. Tuberculous meningitis: many questions, too few answers. *Lancet Neurol* 2005;**4**:160–70.
45. Morgado C, Ruivo N. Imaging meningo-encephalic tuberculosis. *Eur J Radiol* 2005;**55**:188–92.
46. de Castro CC, de Barros NG, Campos ZM, Cerri GG. CT scans of cranial tuberculosis. *Radiol Clin North Am* 1995;**33**:753–69.
47. Jinkins JR, Gupta R, Chang KH, Rodriguez-Carbajal J. MR imaging of central nervous system tuberculosis. *Radiol Clin North Am* 1995;**33**:771–86.
48. Gupta RK, Kathuria MK, Pradhan S. Magnetization transfer MR imaging in CNS tuberculosis. *AJNR Am J Neuroradiol* 1999;**20**:867–75.
49. Gupta RK, Kumar S. Central nervous system tuberculosis. *Neuroimaging Clin N Am* 2011;**21**:795–814.
50. Luthra G, Parihar A, Nath K, Jaiswal S, Prasad KN, Husain N, et al. Comparative evaluation of fungal, tubercular, and pyogenic brain abscesses with conventional and diffusion MR imaging and proton MR spectroscopy. *AJNR Am J Neuroradiol* 2007;**28**:1332–8.
51. Patkar D, Narang J, Yanamandala R, Lawande M, Shah GV. Central nervous system tuberculosis: pathophysiology and imaging findings. *Neuroimaging Clin N Am* 2012;**22**:677–705.
52. Cooper A. Illustrations of the diseases of the breast. Part I. London: Longman, Rees, Orme, Brown and Green; 1829: 73.
53. Al-Marri MR, Almosleh A, Almoslmani Y. Primary tuberculosis of the breast in Qatar: ten year experience and review of the literature. *Eur J Surg* 2000;**166**:687–90.
54. Horn H, Saphir O. The involvement of myocardium in tuberculosis: a review of literature and a report of three cases. *Am Rev Tuberc* 1935;**32**:492–504.
55. Agarwal N, Sharma SK. Concomitant endobronchial tuberculosis, myocarditis and congestive cardiac failure. *Indian J Tuberc* 2000;**47**:169–70.
56. Kubota R, Kubota K, Yamada S, Tada M, Ido T, Tamahashi N. Microautoradiographic study for the differentiation of intratumoral macrophages, granulation tissues and cancer cells by the dynamics of fluorine-18-fluorodeoxyglucose uptake. *J Nucl Med* 1994;**35**:104–12.
57. Stelzmueller I, Huber H, Wunn R, Hodolic M, Mandl M, Lamprecht B, et al. 18F-FDGPET/CT in the initial assessment and for follow-up in patients with tuberculosis. *Clin Nucl Med* 2016;**41**:e187–94.
58. Vorster M, Sathekge MM, Bomanji J. Advances in imaging of tuberculosis: the role of ^{18}F-FDG PET and PET/CT. *Curr Opin Pulm Med* 2014;**20**:287–93.
59. Gambhir S, Kumar M, Ravina M, Bhoi SK, Kalita J, Misra UK. Role of 18FDG PET in demonstrating disease burden in patients with tubercular meningitis. *J Neurol Sci* 2016;**370**:196–200.
60. Sathekge M, Maes A, Van de Wiele C. FDG PET imaging in HIV infection and tuberculosis. *Semin Nucl Med* 2013;**43**:349–66.
61. Kim DW, Kim CG. Dual-time point positron emission tomography findings of benign mediastinal lymph nodes in a tuberculosis-endemic region. *Jpn J Radiol* 2011;**29**:682–7.

Please cite this article in press as: Gambhir S, et al. Imaging in extrapulmonary tuberculosis. Int J Infect Dis (2017), http://dx.doi.org/10.1016/j.ijid.2016.11.003